Biochemical Engineering Journal 90 (2014) 324–332

Contents lists available at ScienceDirect

Biochemical Engineering Journal

journal homepage: www.elsevier.com/locate/bej

Rheological characterization and CFD modeling of corn stover–water mixing system at high solids loading for dilute acid pretreatment

Long-Ping Zhang [1], Jian Zhang [1], Chuan-Hang Li, Jie Bao *

State Key Laboratory of Bioreactor Engineering, East China University of Science and Technology, 130 Meilong Road, Shanghai 200237, China

ARTICLE INFO

Article history:
Received 4 February 2014
Received in revised form 8 June 2014
Accepted 22 June 2014
Available online 28 June 2014

Keywords:
Corn stover
Pretreatment
Rheological properties
Computational fluid dynamics (CFD)
Helical ribbon impeller
High solids content

ABSTRACT

CFD modeling of pretreatment reactors at very high lignocellulose solids content requires the characterization of rheological properties of this specific system. In this study, the non-Newtonian rheological properties of the corn stover–water mixture at high solid loading up to 50% with helical ribbon agitation were characterized. The rheological model was developed by introducing the power law model and measuring the torque values of the mixing system in a small reactor (5 L), and then applied to the larger reactors (50 L and 500 L). The CFD model was developed based on the determined rheological properties. The fluid dynamics experiments in three reactors with different scales were used for validation of the rheological model. The calculated power consumption and mixing efficiency by CFD modeling were in good agreements with the experimental results. This study provided a practical method for the rheology characterization and CFD model at high solids loading. The CFD model could be applied to the design and structure analysis of pretreatment reactors in lignocellulose biorefining processes.

1. Introduction

Pretreatment is the key step of biorefinery processes for overcoming the biorecalcitrance of lignocellulose biomass for consequent hydrolysis by cellulase enzymes [1,2]. Among many pretreatment methods, dilute acid pretreatment is one of the most widely used technologies. However, the traditional dilute acid pretreatment was operated under low solids content, thus significant amount of waste water was generated [3–6]. To overcome this technical barrier, a “dry” pretreatment method was proposed by operating at very high solids/liquid ratio up to 2:1 at the beginning and 1:1 at the end (due to the steam condensation) [6]. When the water content in corn stover is reduced to a very low level, corn stover completely absorb the water leaving no free water. Therefore, the dilute acid pretreatment at very high solids content is called the “dry” method, because both the corn stover feedstock and the pretreated corn stover product are “dry”, without free water during pretreatment: the liquid phase water or solution streams are deleted from the process of this “dry” dilute acid pretreatment.

While the waste water was completely depleted in the dry pretreatment, the intensified mixing of small amount of dilute acid liquid with the lignocellulose solids bulk and steam vapor was strongly required, otherwise the poor mixing leads to the non-uniform distribution of temperature and acid concentration inside the pretreatment reactor. Therefore, the helical ribbon impeller was introduced into pretreatment reactors for the purpose of intensified mixing of corn stover with liquid dilute acid solution and hot steam [7,8]. Robinson and Cleary [9] analyzed the helical ribbon mixer and designed various impellers for a high viscous mixing system. Wu [10] made a comparison of six impellers for mixing high-solids anaerobic digestion systems and found the helical ribbon impeller was the best option. In our previous studies, a helical ribbon impeller was introduced into bioreactors for enzymatic hydrolysis and fermentation, as well as into pretreatment reactors for dry dilute acid pretreatment [11–13]. The results showed that the bioconversion yield and pretreatment efficiency was significantly improved.

Rheological properties of the high solids pretreatment system needs to be developed to design appropriate transport and mixing strategies for high performance with helically agitated mixing. Viamajala et al. [14] studied the rheological properties of pretreated corn stover at the solid content of 10–40% (w/w), which exhibit shear-thinning fluid behavior, but these systems were still in a wet slurry state with high liquid content. Kemblowski and Kristiansen [15] measured the rheological properties of a fermentation broth at high solids content which was still typical liquid slurry. Lavenson et al. [16] used magnetic resonance imaging as an in-line rheometer

* Corresponding author. Tel.: +86 21 64251799; fax: +86 21 64251799.
E-mail address: jbao@ecust.edu.cn (J. Bao).
[1] These authors are equally contributed to this work.

http://dx.doi.org/10.1016/j.bej.2014.06.018
1369-703X/

Notations

d	the impeller diameter (m)
D	the reactor diameter (m)
C	geometric dimension parameter
K_{pl}	consistency coefficient (Pa s^n)
K_s	Metzner constant
l	the immersed height of helical ribbon (m)
M	torque (N m)
n	power-law index
N	the impeller rotation rate (rev/s)
N_p	dimensionless power number
N_r	the number of helical ribbon
P	power consumption (w)
MEL	mixing energy level (W/m^3)
Re_m	Reynolds number (–)
S	pitch size of the helical ribbon (m)
$N_{p\text{-}exp}$	value N_p of experiments
$N_{p\text{-}sim}$	the value N_p of CFD simulation
w	ribbon width (m)

Greek letters

γ_{eff}	apparent shear rate (s^{-1})
μ	viscosity of fluids (Pa s)
η_a	apparent viscosity (Pa s)
ρ	density of fluids (kg/m^3)

to measure velocity profiles and characterize the cellulose suspensions, but the target system was liquid at low solids loading. To the best of our knowledge, no previous studies provided rheological model under solids loading high enough to meet the present dry pretreatment requirement [17–19].

Computational fluid dynamics (CFD) has been used for simulating the mixing performance of high solids loading systems [20,21]. Giuseppina et al. [22] studied the stirred Newtonian and pseudoplastic liquids by CFD simulations and experimental validation of mixing time. Yu et al. [23] developed a numerical method to simulate mixing in high solids digesters using helical ribbon mixers. In their studies, the mixing system contained only 5% solids content and the Newtonian fluid was assumed for the CFD modeling. However, the pretreatment system at very high lignocellulose solids loading up to 50–70% is no longer a Newtonian fluid. A non-Newtonian fluid based rheological model should be established for the high solids system and then used for CFD modeling.

In this study, based on the rheological model, a CFD model was developed to simulate the power consumption and mixing efficiency of corn stover–water system under helical ribbon agitated mixing, which was the initial stage of dry dilute acid pretreatment operation. The specific objectives of this study were to: (i) characterize the rheological properties of high solids loading corn stover–water mixing system; (ii) develop the CFD model based on the newly established rheological model and validate the model by the power consumption and mixing efficiency data; (iii) apply the model to the enlarged reactors for validation and design.

2. Materials and methods

2.1. Raw materials

Corn stover (CS) is selected as the model feedstock material, because it is the most typical lignocellulose biomass from agricultural residues for biofuels and biochemical production by biorefinery processing. The materials were harvested in fall 2010, Jilin, China. The materials were washed to remove the field dirt, stones and metal pieces, and then dried at 105 °C until the weight was constant. Dried corn stover was milled coarsely using a beater pulverizer (SF-300, Ketai Milling Equipment, Shanghai, China) and screened through a sieve with a mesh diameter of 10 mm, then stored in sealed plastic bags until use. The particle size was roughly screened by sample sieves, and the size distribution in average diameter was 26.1% ± 1.4% at the range of less than 0.25 mm, 26.1% ± 0.6% at the range of 0.25–0.42 mm, 27.0% ± 0.8% at 0.42–0.84 mm, 14.6% ± 0.8% at 0.84–2.00 mm, and 6.2% ± 0.6% above 2.00 mm, respectively. All measurements were carried out in triplicate and averaged.

Table 1
Rheological properties of the reference Newtonian fluids.

Fluids	Newtonian fluid	Temperature (°C)	K_{pl} (Pa s)
1	Corn syrup	25.0	6.687
2	Corn syrup	31.0	3.168
3	Glycerol	23.0	1.200
4	Glycerol	27.0	0.844

The glucan and xylan content of corn stover were analyzed using the two-step acid hydrolysis method according to NREL protocol [24,25]. The CS contained 37.2% of glucan, 19.8% of xylan, and 5.5% ash.

Corn syrup and glycerol were used as reference Newtonian fluids in the experiments. Corn syrup and glycerol were purchased from Haocheng Food Co., Shanghai, China, and the rheological parameters of the fluids are listed in Table 1. The reference Newtonian fluids were used for the determination of the geometry dependent parameters of the reactors.

2.2. Pilot reactors and rheological parameters measurement

The schematic diagram of the three pilot reactors is shown in Fig. 2(a). The reactors were made by PMMA polymer material. The helical ribbon impeller was welded on the central shaft, and the motor was mounted on the top of the impeller to form axial upwelling flow. The torque meter HX-901 (Huaxin Mechanical and Electrics Co., Beijing, China) was installed onto each of the three pilot reactors for the measurement of agitation torque. The temperature change from mechanical friction during the mixing was ignored.

In the three reactors, 150 g, 1.50 kg, and 15.0 kg of corn stover (dry base) was charged onto the Reactors A, B, and C, respectively. Tap water was poured onto the bottom of Reactor A before the corn stover materials were fed. For Reactors B and C, tap water was fed from the top of Reactors B and C after the materials were charged. The torque was recorded every 5 s for 8–10 min at each agitation rate in the range of 50–110 rpm. The mean torque value was calculated and recorded as T_i. The zero torque value with empty feeding was recorded as T_{i0}. The true torque value on mixing M was defined as $M = T_i - T_{i0}$. The power consumption P was calculated by Eq. (1):

$$P = \frac{(T_i - T_{i0}) \times 2\pi \times \nu}{60} \quad (1)$$

where ν is the impeller agitation rate (rpm).

The mixing efficiency was characterized by monitoring the water content in corn stover during mixing. One difficulty of the experiment is the choice of tracer in characterizing the mixing of corn stover and water because of the high absorption property of corn stover to any liquid tracers. The tracer selected in this study is water and the water content in the corn stover slurry system is measured periodically. The purpose of water addition from the top of the reactors is to mimic the co-currently addition of dilute acid solution with corn stover feedstock in the practical operation [8].

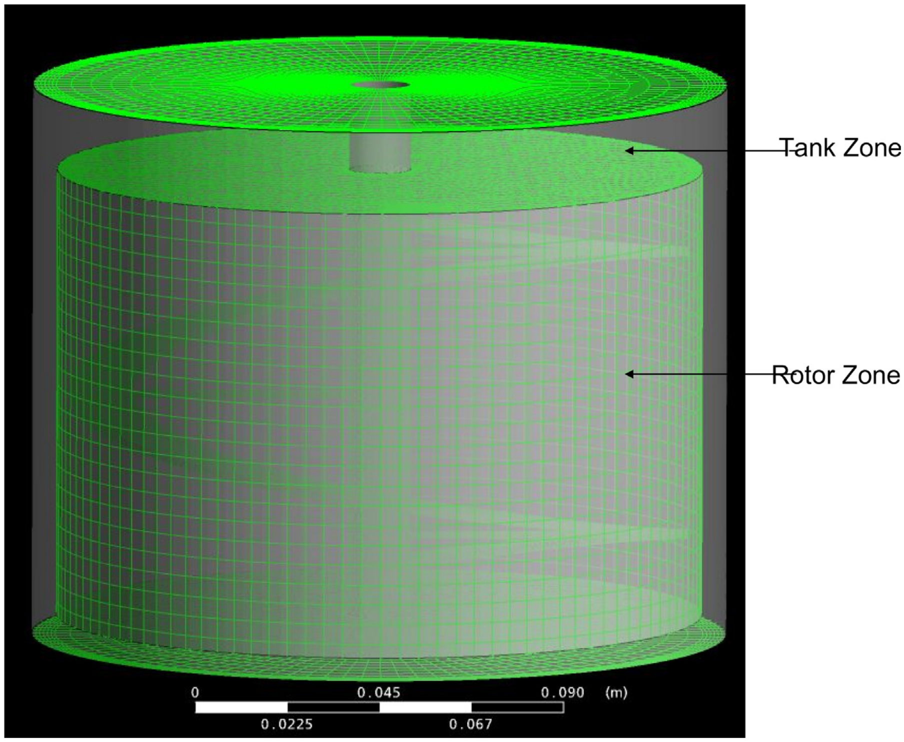

Fig. 1. Grids resolution of rotor and tank zone in ICEM CFD. The Rotor Zone contains the helical ribbon impeller.

The power consumption was characterized by measuring the torque of the mixing at different conditions. 1.0 g of the samples was withdrawn from the reactors at the upper middle location of the impeller every 30 s and lasted for 720 s, and weighed as m_1. The volume change by sampling was less than 1% of the total volume. The sample was dried at 105 °C until the weight was constant, then weighed as m_2. The water content of each sample was calculated by

$$W\% = \frac{m_1 - m_2}{m_1} \times 100\% \tag{2}$$

The water content of the samples was normalized by dividing the theoretical water content (calculated based on the total added water and the corn stover). The corn stover suspension was slowly discharged from the bottom valve while the agitation was still kept on, because the high solids containing suspension was unable to be transported by pumps.

2.3. CFD modeling

A commercial grid-generation tool, ICEM CFD 11.0 (Ansys Inc., US) was used to generate the 3D grids of the reactor model created in Solidworks 2010 (Dassault Inc., France). The mathematical model, in which the impeller rotation was characterized with the Multiple Reference Frame model (MRF), was solved in CFX 11.0. The initial and boundary conditions were specified as:

(1) The impeller and shaft regions are stationary to the fluid body in the agitation region;
(2) No slip wall effect;
(3) The tracer has the same physical properties as the background fluid, and no chemical reaction occurs;
(4) The mass fraction of the tracer in the injected area equaled to 1 at the beginning of the agitation while at all other areas equaled to 0.

Among the assumptions, the wall-depletion phenomenon is inevitable in the practical mixing of corn stover–water system, which leads to the predict errors for power consumption calculation and mixing time. Therefore, the mock-up experiment is carried out to estimate the predict errors for this corn stover–water system.

The 3-D grids of the helically agitated reactor were using structured grids except for the rotor zone that contains the impeller. The mesh was relatively fine near the impeller blades and coarser far away from the impeller. Tetrahedral mesh in the rotor zone and hexahedral mesh in the tank zone were used as shown in Fig. 1.

For evaluation the mixing efficiency with the transient state calculation, the uniformly distributed 12 monitoring points inside the reactors were chosen for monitoring the tracer concentration, where the locations are shown in Fig. 2(b). The prediction of mixing time for the non-Newtonian fluids was not affected by the exact locations of monitoring points and tracer injection, which was verified in the study of Giuseppina et al. [22]. Then, degree of homogeneity ($M(t)$) was defined as:

$$M(t) = \frac{\left|c_i(t) - c_{ave}\right|}{c_{ave}} \times 100\% \qquad M(t) \leq 5\% \tag{3}$$

where $c_i(t)$ is the tracer concentration, and c_{ave} is the average tracer concentration throughout the entire computational domain. The mixing time was defined as the time required to achieve $M(t) \leq 5\%$.

3. Results and discussion

3.1. Determination of apparent viscosity η_a of corn stover–water mixing system

A CFD model requires the rheological parameters of the mixing system. In this study, the scattered corn stover particles were assumed to form fluid-like suspensions and their rheological properties were determined by measuring the torque value at different

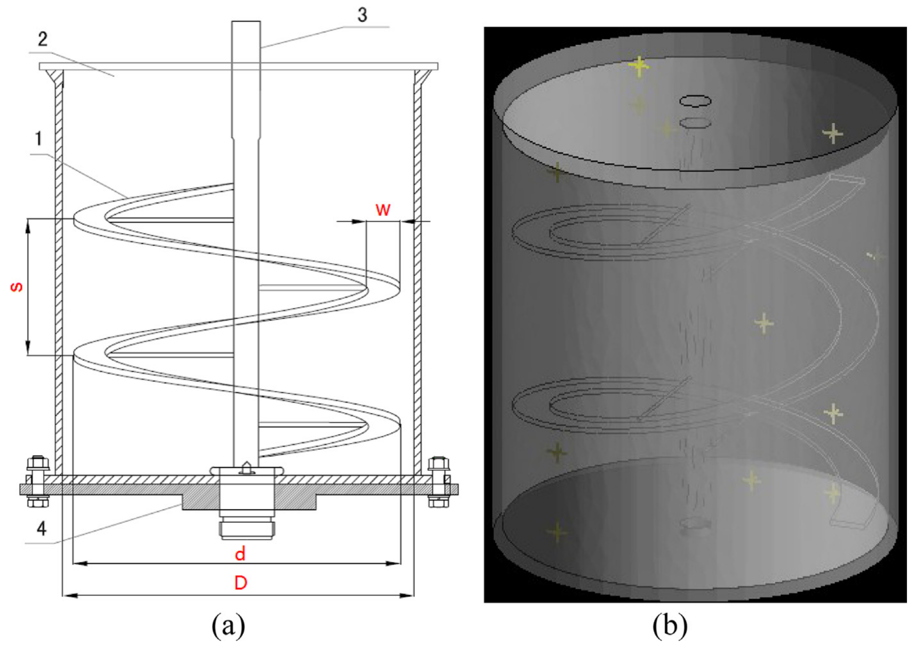

Fig. 2. Schematic diagram of the mock-up reactors. (a) Dimension of reactors: 1 – single helical ribbon impeller; 2 – material inlet; 3 – agitating shaft for driving the helical ribbon impeller; 4 – material outlet. *d* is the outer-diameter of the helical impeller; *D* is the inner-diameter of the reactor; *w* is the thickness of the helical impeller; *s* is the pitch size of the helical impeller; N_r is the coil number of the helical impeller. (b) Locations of 12 monitoring points for tracer concentration in the CFD model.

operating conditions [26–28]. The rheological properties were firstly determined in a 5 L helically agitated Reactor A as shown in Fig. 2, then applied to the larger reactors and CFD modeling because the rheological properties are independent of the mixing vessel size.

The first step toward the rheological properties measurement is to develop the method of apparent viscosity η_a determination for the corn stover–water system in Reactor A. The dimensionless power number N_p was expressed as the function of Reynolds number Re_m under the laminar flow [29]:

$$N_p = C \cdot Re_m^x \tag{4}$$

or its logarithm form:

$$\log_{10} N_p = \log_{10} C + x \cdot \log_{10}\ Re_m \tag{5}$$

where *C* is a geometry parameter of the reactor used and independent of the fluid properties, *x* is a dimensionless factor.

The Newtonian fluid assumption apparently no longer fitted the corn stover–water mixing system at high solids content. Therefore, the Re_m value for a non-Newtonian fluid system under laminar flow condition ($Re_m < 300$) was calculated by Eq. (6) according to Chen [30]:

$$Re_m = \frac{\rho N d^2}{\eta_a} \tag{6}$$

where ρ is the density of the fluid (kg/m^3), *N* is the impeller rotation rate (rev/s), *d* is the impeller diameter (m), η_a is the apparent viscosity (Pa s). Here, ρ, *N*, *d*, and η_a are all measurable parameters for the mixing system for Reactor A.

The N_p value under different rotation rate in Reactor A was calculated by Eq. (7) according to Paul et al. [31]:

$$N_p = \frac{P}{\rho N^3 d^5} \tag{7}$$

where *P* was the power consumption of stirred impeller (*W*), and could be represented as:

$$P = 2\pi N M \tag{8}$$

where *M* was the torque of the impeller (N m). Thus inserting Eq. (8) into Eq. (7) gives Eq. (7a) for calculation of N_p using measurable parameters M, ρ, *N*, and *d*:

$$N_p = \frac{P}{\rho N^3 d^5} = \frac{2\pi N M}{\rho N^3 d^5} = \frac{2\pi M}{\rho N^2 d^5} \tag{7a}$$

Based on the working equation Eq. (5), the correlation of $\log_{10}N_p$–$\log_{10}Re_m$ for the helical ribbon impeller in Reactor A was plotted using four different Newtonian fluids (corn syrup and glycerol at different temperatures) as shown in Fig. 3. The results show that the maximum $\log_{10}Re_m$ was less than 2.0 under the experimental conditions, therefore the laminar flow assumption in Eqs. (4)–(6) were valid ($Re_m < 300$).

Fig. 3 indicates that the $\log_{10}N_p$–$\log_{10}Re_m$ plots of the four fluids were linear and could be perfectly fitted into one correlation. The slope and intercept corresponded to *x* and $\log_{10} C$ in Eq. (5) were

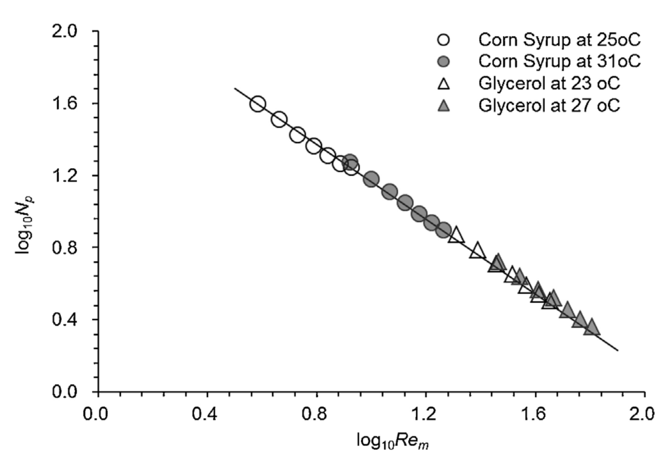

Fig. 3. Logarithmic graphs of the power number N_p versus Reynolds number Re_m in Reactor A. Two Newtonian fluids, corn syrup and glycerol were used in the measurement of the structure parameter *C*.

determined as $x = -1$ and $C = 147.12$. Thus Eq. (5) was simplified into:

$$N_p = \frac{147.12}{Re_m} \tag{9}$$

Eqs. (6), (7a) and (9) gives Eq. (10) for calculation of the apparent viscosity η_a using the measurable parameters M, N, and d in Reactor A:

$$\eta_a = \frac{2\pi M}{CNd^3} = \frac{\pi M}{73.56Nd^3} \tag{10}$$

3.2. Determination of rheological parameters of corn stover–water mixing system

The power-law model was used to describe the non-Newtonian properties of corn stover–water mixing system:

$$\eta_a = K_{pl} \cdot \gamma_{eff}^{n-1} \tag{11}$$

where K_{pl} was the consistency coefficient (Pa s^n), n was the dimensionless power-law index, γ_{eff} was the apparent shear rate (s^{-1}) and expressed according to Metzner and Otto [32]:

$$\gamma_{eff} = K_s \cdot N \tag{12}$$

where K_s was the Metzner constant, N was the impeller speed (rev/s). Then, Eqs. (11) and (12) gives the working equation for determination of the rheological parameters K_{pl} and n:

$$\eta_a = K_{pl} \cdot \gamma_{eff}^{n-1} = K_{pl} \cdot (K_s \cdot N)^{n-1} \tag{13}$$

or

$$\log_{10} \eta_a = \log_{10} K_{pl} + (n-1) \cdot \log_{10}(K_s \cdot N) \tag{13a}$$

For a specific stirred tank and fluid, K_s value was constant and the power-law index n was calculated by determining the apparent viscosity η_a at different agitation rate (N_1, N_2):

$$n - 1 = \frac{\log_{10}\eta_{a1} - \log_{10}\eta_{a2}}{\log_{10}(K_s \cdot N_1) - \log_{10}(K_s \cdot N_2)} = \frac{\log_{10}\eta_{a1} - \log_{10}\eta_{a2}}{\log_{10}N_1 - \log_{10}N_2} \tag{14}$$

According to Delaplace et al. [33], the K_s value can be calculated by Eq. (15) for the helical impeller in the range of $0 < n < 0.45$:

$$K_s = \frac{2}{N_r}\frac{S^{2/n}}{S^2}\frac{S_e^2 - 1}{S_e^{2/n} - 1}\frac{C}{\pi^2(l/d)} \cdot \left[\frac{n}{2-n}\frac{S^{(2/n)-1}}{S-1}\right]^{1/(n-1)} \tag{15}$$

$$S_e = \frac{D}{d_e} = \frac{D/d}{(D/d) - 2w/d/(\ln((D/d) - (1 - 2w/d)/D/d - 1))} \tag{16}$$

where S is the diameter ratio of D/d of the helical ribbon impeller, w is ribbon width (m), d is the impeller diameter (m), l is the immersed height of helical ribbon (m), D is the reactor diameter (m), N_r is the number of helical ribbon. The dimension of the helical impeller should satisfy the following condition: $N_r = 1$ or 2, $0.025 < D/d < 0.263$, $0.084 < w/d < 0.223$, $0.35 < s/d < 2.15$.

Fig. 4 shows the correlations of $\log_{10}\eta_a$–$\log_{10}\gamma_{eff}$ of the pseudo-fluid of corn stover–water mixing flow at different water content from 0% to 60% based on the working equation Eq. (13a). The satisfactory linear correlations were obtained for all the samples measured. The rheological parameters K_{pl} and n values obtained are shown in Table 2. The n values at all water levels were in the range of $0.168 < n < 0.425$, which fell within the range of $0 < n < 0.45$ assumed in Eqs. (15) and (16), indicating that the K_s value in Eq. (13) can be calculated using Eqs. (15) and (16). With the increasing corn stover solids content from 0% to 20%, the n values decreased quickly from 0.425 to 0.261, indicating the strong shear-thinning behavior of corn stover–water mixing system at the low water content. Dunaway et al. [34] also reported that the slurries of pretreated corn stover at 25% of solids content exhibited the shear-thinning fluid characteristics. Then the n values maintained relatively unchanged around 0.2 with further increasing water content from 20% to 60%. On the other hand, the K_{pl} values obtained were found to constantly increase from 5.9 to 41.2 with the decreasing water content from 0% to 60%, indicating the increased viscosity of corn stover–water mixing system with the increasing water content. The rheological parameters K_{pl} and n measured in Reactor A (5 L) were independent of vessel size, if the maximum Re_m in the enlarged reactors was below 300 for validation of Eq. (6). The maximum Re_m for the three reactors was 259.78 at 50% water content and 110 rpm agitation in Reactor C, thus the rheological parameters could be applied to the fluid dynamic calculation for the enlarged reactors B (50 L) and C (500 L), as well as CFD modeling for industrial scale reactors mixed with the helical ribbon impeller.

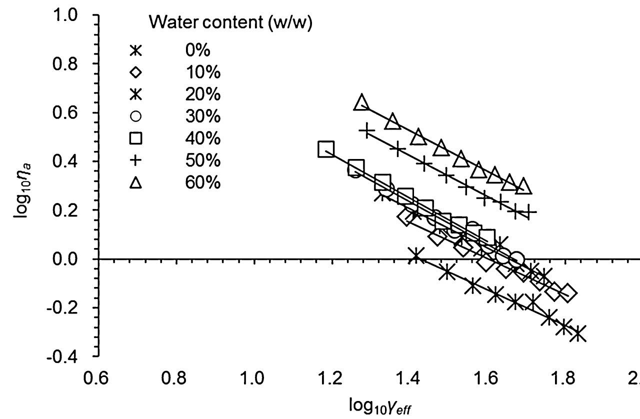

Fig. 4. Logarithmic of the apparent viscosity η_a as a funcation of logarithmic of the apparent shear rate γ_{eff}. Water content represented the water content of corn stover–water mixing system (w/w).

The traditional view on rigid solids containing fluid suggests that the viscosity decreases with increasing water content due to the lubricating effect of water added. However, for soft and long lignocellulose solids with filamentous fiber morphology, the rheological properties behave differently. Fig. 4 shows the apparent viscosity η_a as a function of the apparent shear rate γ_{eff} at six different water contents from 0% to 60%. Opposite to the rigid solids containing fluid, the apparent viscosity η_a of the corn stover–water suspensions increased, instead of decreased, with increasing water content in the range of 0–60% (w/w) water. The reason of this unusual phenomenon should come from the unique properties of corn stover materials. Corn stover absorbs water immediately and completely after its addition in the range up to 60% of water. Thus, the water added is unable to act as lubricant to reduce the viscosity of the corn stover–water suspension. Instead, the filamentous corn stover fibers are swelled by water absorbed and the

Table 2
Rheological properties of corn stover–water mixing system at 25 °C.

Water content (%, w/w)	n (–)	K_{pl} (Pa s^n)
0	0.425 ± 0.010	5.914 ± 0.337
10	0.356 ± 0.027	12.078 ± 1.165
20	0.261 ± 0.027	17.990 ± 2.153
30	0.204 ± 0.012	21.419 ± 1.440
40	0.168 ± 0.021	27.188 ± 1.322
50	0.225 ± 0.011	32.041 ± 1.200
60	0.215 ± 0.026	41.197 ± 1.757

Table 3
Grids independence validation and effect of elements on the power number.

Case		Elements	$N_{p\text{-}sim}$	$(N_{p\text{-}sim}-N_{p\text{-}exp})/N_{p\text{-}exp}$
Reactor A	1	89,387	41.47	4.83%
	2	167,515	41.36	4.55%
	3	326,738	41.25	4.17%
Reactor B	1	102,754	25.75	4.32%
	2	182,452	25.58	3.65%
	3	293,645	25.40	2.93%
Reactor C	1	347,852	6.86	4.98%
	2	510,246	6.80	4.12%
	3	864,751	6.74	3.25%

Element is the number of CFD grid cells for each model. $N_{p\text{-}sim}$ is the value N_p of CFD simulation, $N_{p\text{-}exp}$ is the value N_p of experiments.

intertwined entanglement of the filamentous fibers is further enhanced. The swelling and entangling of corn stover materials lead to the increased friction among swelled and intertwined fibers. As the result, the observed rheological performance is the increase of the apparent viscosity of the corn stover suspension at high solids content. It is expected that the intercross entanglement of the swelled corn stover fibers will be loosed gradually to singular particles with the further increase of water addition to diluted suspensions, and then the rheological performance will be similar to that of the rigid solids containing fluid system. This is an interesting phenomenon and worth further investigation in the future studies.

3.3. CFD modeling using the rheological parameters and its validation

The CFD model of corn stover–water mixing system was established using CFX platform based on the rheological properties determined above (Table 2). The grid independence of CFD model were tested by comparing the power number N_p between the CFD calculation and the experimental data of the three reactors, Reactors A (5 L), B (50 L), and C (500 L). The N_p values of the three pilot reactors were determined as 39.58 (Reactor A), 24.68 (Reactor B) and 6.53 (Reactor C), respectively, using corn syrup at 25 °C and 50 rpm as the reference fluid. Table 3 shows that the comparison of the experimental N_p values and the N_p under different mesh quality. A moderate grid quantity, 167,515 for Reactor A, 182,452 for Reactor B and 510,246 for Reactor C, respectively, should be satisfied for the CFD model with the relative deviation of 3–5%.

The calculated power consumption by CFD modeling was compared with the experimental results under varying operating conditions for the validation of rheological parameters determined. The power consumptions in Reactor A at varying water content from 0% to 60% and agitation rate from 50 to 100 rpm were recorded as the experimental results. The comparison of the experimental and calculated power consumptions were shown in Fig. 5. The results show that the calculated values roughly agreed with experimental values under different operation conditions with the relative deviations less than 5%.

For the further validation of the rheological properties and CFD model, the calculated power consumptions in the enlarged reactors (Reactors B and C) were compared with the experimental results at fixed water content of 50% and varying agitation rate from 50 to 110 rpm as shown in Fig. 6. The results indicate that the calculated power consumption again roughly agreed with the experimental ones, with calculated power consumption slightly greater than the experimental ones, but the maximum relative deviation was less than 10%.

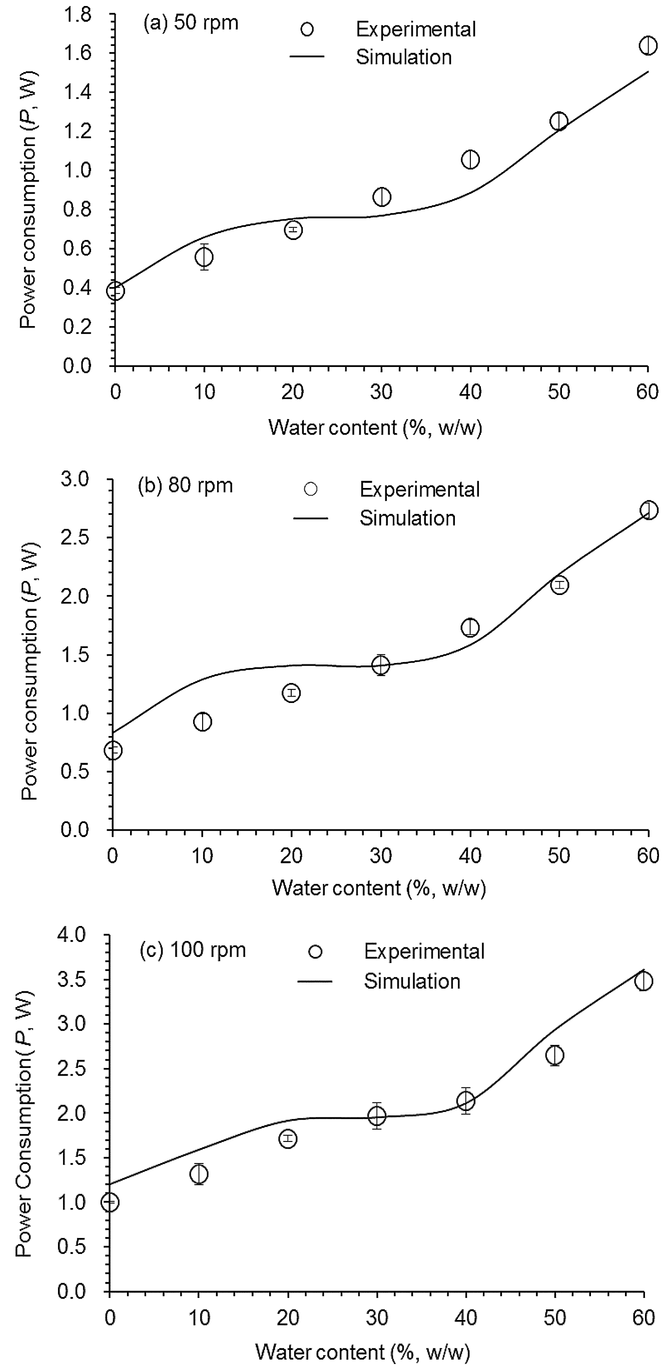

Fig. 5. Comparison of the power consumption between CFD simulations and the mock-up experiments. Conditions: corn stover with different water content (from 0% to 60%), agitation rate at (a) 50 rpm, (b) 80 rpm, and (c) 100 rpm in Reactor A.

3.4. CFD prediction of mixing efficiency of CS-water mixing system

After the CFD model was validated for power consumption calculation, the mixing efficiency of corn stover–water mixing system was engaged in the experiments and calculated for further validation of CFD model. The mixing experiments of corn stover and water were carried out in the three reactors at a fixed agitation rate of 50 rpm. Water was fed into the reactors at the beginning until it reached 50% (w/w). In the CFD modeling, the model was set up as a steady state model thus the water content was set to 50% directly without considering the dynamic process of water feeding.

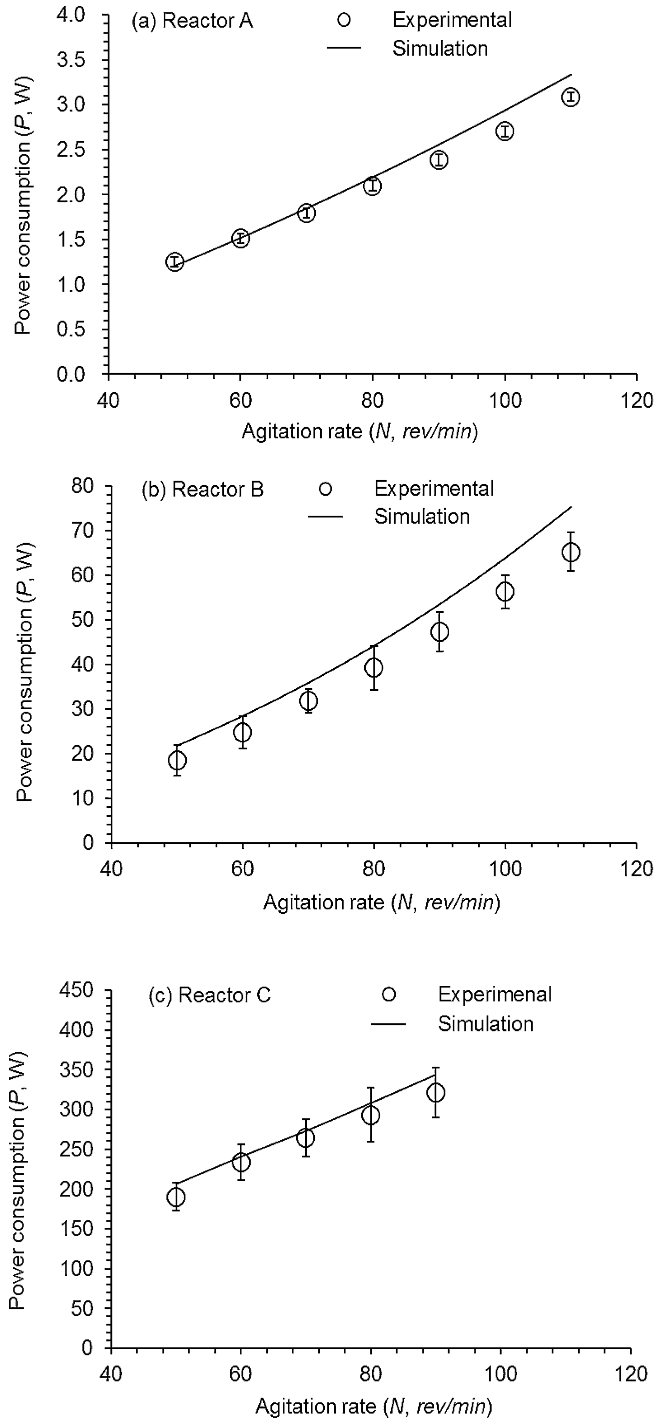

Fig. 6. Comparison of the power consumption between CFD simulations and the mock-up experiments in the three mock-up reactors. Conditions: corn stover with 50% water content, agitation rate from 50 rpm to 110 rpm in Reactor A, Reactor B and Reactor C.

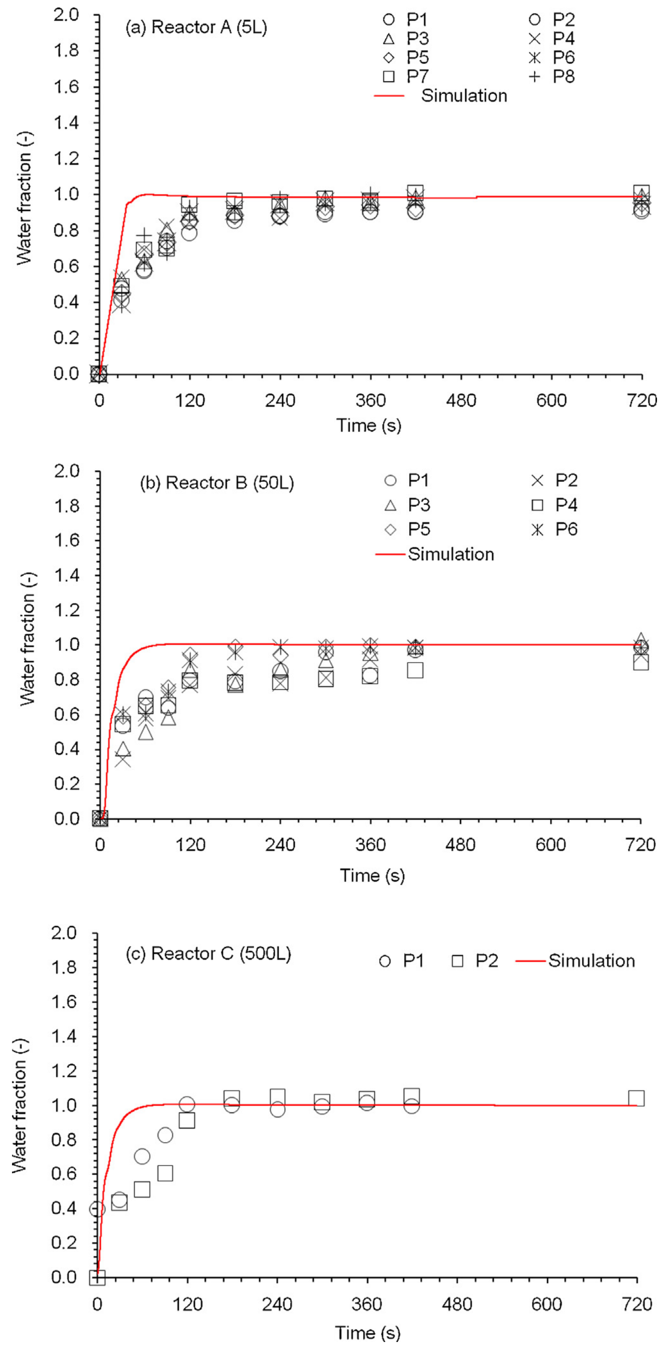

Fig. 7. Comparison of response curves between CFD simulations and mixing experiments. CFD models monitored the tracer concentration at the same location with sampling, and experiments monitored the water fraction of CS during mixing. Both the concentration of CFD simulations and experiments were normalized by dividing the final concentration. All the agitation rate was 50 rpm, which was equal to the actual pretreatment, P1–P8 were differently repeated experiments, and CFD models used the rheological parameter of 50% water content CS.

The tracer concentration was the average of 4 monitoring points, which were symmetrical distribution and at the same horizontal cycle with sampling location. The method may lead to less difference in operating mode between CFD calculation and experiments.

Fig. 7 shows the comparison of mixing efficiency between the experimental and CFD calculated results at 50 rpm and 50% water fraction in three reactors, Reactors A (5 L), B (50 L), and C (500 L). In the initial stage of calculation curve, the tracer concentration in each CFD calculation was all greater than that for the experiment. These results were normal for the experimental mixing, because the tracer (water) concentration showed the average water fraction, and the water transfer rate in the high solids loading system was lower than that in continuous liquid phase. However, Fig. 7 still shows that the overall calculated mixing time agreed with the experimental ones in all the three reactors, approximately 120–180 s.

After the CFD model was validated for power consumption and mixing efficiency calculations, the mixing energy level (*MEL*) ($MEL = P/V$, where V was the working volume of reactor) and mixing time was predicted by the CFD model. Table 4 shows that although

Table 4
CFD calculation of mixing energy level (*MEL*) and mixing time of the three reactors.

Water content (%, w/w)	Reactor A		Reactor B		Reactor C	
	MEL (W/m^3)	Mixing time (s)	*MEL* (W/m^3)	Mixing time (s)	*MEL* (W/m^3)	Mixing time (s)
0	78.02	58.56	163.34	60.96	200.46	46.32
10	130.38	61.56	251.67	69.36	271.86	47.52
20	149.64	68.76	284.73	75.60	293.56	57.48
30	153.21	80.76	290.93	81.84	295.48	64.80
40	176.56	94.80	330.00	89.76	324.66	66.60
50	239.91	78.24	435.96	84.60	412.64	63.84
60	299.60	82.08	535.54	87.24	491.18	67.32

All the CFD simulations used rheological parameters of corn stover–water mixing system in Table 2.

generally *MEL* and mixing time increased with the decreasing solids content and reactor scales, the increasing tendency varied with the reactor scales. At a typical agitation rate of 50 rpm, the mixing time of the largest reactor C was 63.84 s, which was shorter than that of smaller reactors, Reactor A and B (78.24 s and 84.60 s, respectively), indicating that the mixing efficiency might be enhanced with the increased reactor scale due to the greater radial and tangential velocities of the helical ribbon impeller in the larger reactors. The similar *MEL* values were maintained in Reactor B and C (435.96 and 412.64 W/m^3, respectively), indicating that the *MEL* value did not always increase with the increased reactor scale and a maximum turning point might be reached with the increasing reactor scale for power consumption. These results suggest that a carefully designed reactor structure by CFD modeling may provide an optimum with the maximum mixing efficiency the minimum power consumption for corn stover–water mixing system. However, the further design on the structure of scale-up reactors and analysis of the helical ribbon impeller were in progress, these work focused on developing the rheological model and validating the power consumption and mixing efficiency of the CFD model.

The purpose of this study is to provide the methodology for designing the pretreatment reactor of dry dilute acid pretreatment of corn stover materials. The methodology of rheology measurement and CFD modeling certainly stand for any other lignocellulose feedstocks, but it is less possible that the parameter values of the present corn stover system remain at the same. The rheological values depend on various properties of biomass used, such as the biomass type, size distribution, fiber length, etc., and have to be measured experimentally when the specific pretreatment conditions are given. It is also possible that the agricultural residues, such as corn stover, rice straw, wheat straw, may show some similarity in their rheological properties values, especially for feedstocks with similar size distribution, based on the fact that their pretreatment efficiency is approximately the same [6].

4. Conclusion

The rheological properties of the corn stover–water mixture at very high solid loading up to 50% with helical ribbon agitation were characterized. The power law model was introduced by measuring the torque values of the mixing system in a small reactor (5 L), and then applied to the larger reactors (50 L and 500 L). The CFD model was developed based on the rheological properties. The experiment of corn stover–water mixing system at high solids loading was carried out in three reactors with different scales. The experimental results were in good agreements with the CFD calculated ones. The method of rheology characterization and CFD modeling can be applied to other lignocellulosic material system at high solids loading system.

Acknowledgements

This research was supported by the National Basic Research Program of China (2011CB707406), the National High-Tech Program of China (2012AA022301/2014AA021901), the Natural Science Foundation of China (21306048), and the Fundamental Research Funds for the Central Universities of China (WF1214025).

References

[1] M. Galbe, G. Zacchi, Pretreatment of lignocellulosic materials for efficient bioethanol production, Adv. Biochem. Eng. Biotechnol. 108 (2007) 41–65.
[2] B. Yang, C. Wyman, Pretreatment: the key to unlocking low-cost cellulosic ethanol, Biofuels Bioprod. Bioref. 2 (2008) 26–40.
[3] B.C. Saha, L.B. Iten, M.A. Cotta, Y.V. Wu, Dilute acid pretreatment, enzymatic saccharification and fermentation of wheat straw to ethanol, Process Biochem. 40 (2005) 3693–3700.
[4] C.E. Wyman, B.E. Dale, R.T. Elander, M. Holtzapple, M.R. Ladisch, Y.Y. Lee, Coordinated development of leading biomass pretreatment technologies, Bioresour. Technol. 96 (2005) 1959–1966.
[5] D. Humbird, R. Davis, L. Tao, C. Kinchin, D. Hsu, A. Aden, Process Design and Economics for Biochemical Conversion of Lignocellulosic Biomass to Ethanol: Dilute-acid Pretreatment and Enzymatic Hydrolysis of Corn Stover, National Renewable Energy Laboratory, Golden, CO, 2011.
[6] J. Zhang, X.S. Wang, D.Q. Chu, Y.Q. He, J. Bao, Dry pretreatment of lignocellulose with extremely low steam and water usage for bioethanol production, Bioresour. Technol. 102 (2011) 4480–4488.
[7] Y. He, L. Zhang, J. Zhang, J. Bao, Helically agitated mixing in dry dilute acid pretreatment enhances the bioconversion of corn stover into ethanol, Biotechnol. Biofuels 7 (2014) 1.
[8] Y. He, J. Jian Zhang, J. Bao, Dry dilute acid pretreatment by co-currently feeding of corn stover feedstock and dilute acid solution without impregnation, Bioresour. Technol. 1 (158) (2014) 360–364.
[9] M. Robinson, P.W. Cleary, Flow and mixing performance in helical ribbon mixers, Chem. Eng. Sci. 84 (2012) 382–398.
[10] B.X. Wu, CFD simulation of mixing for high-solids anaerobic digestion, Biotechnol. Bioeng. 109 (2012) 2116–2126.
[11] J. Zhang, D.Q. Chu, J. Huang, Z.C. Yu, G.C. Dai, J. Bao, Simultaneous saccharification and ethanol fermentation at high corn stover solids loading in a helical stirring bioreactor, Biotechnol. Bioeng. 105 (2010) 718–728.
[12] W. Liu, Y.M. Wang, Z.C. Yu, J. Bao, Simultaneous saccharification and microbial lipid fermentation of corn stover by oleaginous yeast *Trichosporon cutaneum*, Bioresour. Technol. 118 (2012) 13–18.
[13] K. Zhao, Q.A. Qiao, D.Q. Chu, H.Q. Gu, T.H. Dao, J. Zhang, J. Bao, Simultaneous saccharification and high titer lactic acid fermentation of corn stover using a newly isolated lactic acid bacterium *Pediococcus acidilactici* DQ2, Bioresour. Technol. 135 (2013) 481–489.
[14] K. Viamajala, J.D. Mcmillan, D.J. Schell, R.T. Elander, Rheology of corn stover slurries at high solids concentrations: effects of saccharification and particle size, Bioresour. Technol. 100 (2009) 925–934.
[15] Z. Kemblowski, B. Kristiansen, Rheometry of fermentation liquids, Biotechnol. Bioeng. 28 (1986) 1474–1483.
[16] D.M. Lavenson, E.J. Tozzi, M.J. McCarthy, R.L. Powell, Yield stress of pretreated corn stover suspensions using magnetic resonance imaging, Biotechnol. Bioeng. 108 (2011) 2312–2319.
[17] Y. Haroun, Y. Raynal, D. Legendre, Mass transfer and liquid hold-up determination in structured packing by CFD, Chem. Eng. Sci. 75 (2012) 342–348.
[18] J. Knutsen, M. Liberatore, Rheology of high-solids biomass slurries for biorefinery applications, J. Rheol. 53 (2009) 877–893.
[19] M. Wiman, B. Palmqvist, E. Tornberg, G. Liden, Rheological characterization of dilute acid pretreated softwood, Biotechnol. Bioeng. 108 (2011) 1031–1041.

[20] A.D. Renzo, D.F.P. Maio, Homogeneous and bubbling fluidization regimes in DEM-CFD simulations: hydrodynamic stability of gas and liquid beds, Chem. Eng. Sci. 62 (2007) 116–130.
[21] F. Habla, H. Marschall, O. Hinrichsen, L. Dietsche, H. Jasak, J.L. Favero, Numerical simulation of viscoelastic two-phase flows using open FOAM, Chem. Eng. Sci. 66 (2011) 5487–5496.
[22] M. Giuseppina, M. Michal, J. Milan, M. Franco, CFD simulations and experimental validation of homogenization curves and mixing time in stirred Newtonian and pseudoplastic liquids, Chem. Eng. Sci. 60 (2005) 2427–2437.
[23] L. Yu, j. Ma, S. Chen, Numerical simulation of mechanical mixing in high solid anaerobic digester, Bioresour. Technol. 102 (2011) 1012–1018.
[24] A. Sluiter, B. Hames, R. Ruiz, C. Scarlat, J. Sluiter, D. Templeton, D. Crocker, Determination of Structural Carbohydrates and Lignin in Biomass, National Renewable Energy Laboratory, Golden, CO, 2008.
[25] A. Sluiter, B. Hames, R. Ruiz, C. Scarlata, J. Sluiter, D. Templeton, Determination of Sugars, Byproducts, and Degradation Products in Liquid Fraction Process Samples, National Renewable Energy Laboratory, Golden, CO, 2008.
[26] V.V. Ranade, J.R. Bourne, J.B. Joshi, Fluid mechanics and blending in agitated tanks, Chem. Eng. Sci. 46 (1991) 1883–1893.
[27] J.J. Stickel, R.L. Powell, Fluid mechanics and rheology of dense suspensions, Annu. Rev. Fluid Mech. 37 (2005) 129–149.
[28] J.C. Gabelle, E. Jourdier, R.B. Licht, F.B. Chaabane, I. Henaut, J. Morchain, F. Augier, Impact of rheology on the mass transfer coefficient during the growth phase of *Trichoderma reesei* in stirred bioreactors, Chem. Eng. Sci. 75 (2012) 408–417.
[29] P.J. Carreau, R.P. Chhabra, J. Cheng, Effect of rheological properties on power consumption with helical ribbon agitators, AIChE J. 39 (1993) 1421–1430.
[30] Y.R. Chen, Impeller power consumption in mixing livestock manure slurries, Trans. ASAE 24 (1981) 187–192.
[31] E.L. Paul, V.A. Atiemo-Obeng, S.M. Kresta, Handbook of Industrial Mixing, John Wiley Sons, New Jersey, 2004.
[32] A.B. Metzner, R.E. Otto, Agitation of non-Newtonian fluids, AIChE J. 3 (1957) 3–10.
[33] G. Delaplace, R. Guerin, J. Leuliet, R.P. Chhabra, An analytical model for the prediction of power consumption for shear-thinning fluids with helical ribbon and helical screw ribbon impellers, Chem. Eng. Sci. 61 (2006) 3250–3259.
[34] K.W. Dunaway, R.K. Dasari, N.G. Bennett, R.E. Berson, Characterization of changes in viscosity and insoluble solids content during enzymatic saccharification of pretreated corn stover slurries, Bioresour. Technol. 101 (2010) 3575–3582.